Eur. Phys. J. D **33**, 421–432 (2005)
DOI: 10.1140/epjd/e2005-00070-4

THE EUROPEAN PHYSICAL JOURNAL D

Structure and dynamics of cationic van-der-Waals clusters

I. Binding and structure of protonated argon clusters

T. Ritschel[1], P.J. Kuntz[2], and L. Zülicke[1,a]

[1] Universität Potsdam, Institut für Chemie, Karl-Liebknecht-Straße 24-25, 14476 Golm, Germany
[2] Hahn-Meitner-Institut, Abteilung SF5, Glienicker Straße 100, 14109 Berlin, Germany

Received 14 February 2005
Published online 24 May 2005 –

Abstract. The geometric structure and bonding properties of medium-sized Ar_nH^+ clusters (n = 2–35), in which a proton is wrapped up in a number of Ar atoms, are investigated by applying a diatomics-in-molecules (DIM) model with ab-initio input data generated by means of multi-reference configuration-interaction (MRCI) computations. For the smaller complexes, n = 2–7, cross-checking calculations employing the coupled-cluster approach (CCSD) with the same one-electron atomic basis set as for the input data calculations (aug-cc-pVTZ from Dunning), show good agreement thus justifying the extension of the DIM study to larger n. Local minima of the multi-dimensional potential-energy surfaces (PES) are determined by combining a Monte-Carlo sampling followed, for each generated point, by a steepest-descent optimization procedure. For the electronic ground state of the Ar_nH^+ clusters, the global minimum (corresponding to the most stable structure of the cluster) as well as secondary minima are found and analyzed. The structural and energetic data obtained reveal the building-up regularities for the most stable structures and make it possible to formulate a simple increment scheme. The low-lying excited states are also calculated by the DIM approach; they all turn out to be globally repulsive.

PACS. 31.15.Ar Ab initio calculations – 31.50.Bc Potential energy surfaces for ground electronic states – 31.50.Df Potential energy surfaces for excited electronic states – 36.40.-c Atomic and molecular clusters – 36.40.Wa Charged clusters – 36.40.Qv Stability and fragmentation of clusters

1 Introduction

Positively charged clusters of the type Rg_nM^+, where Rg denotes a rare-gas atom and M some atom or diatomic molecule, have become the subject of increasing research activity in the recent two decades (for general information see, e.g., [1, 2]). The reasons for this interest are of various kinds. First of all, compared with their neutral counterparts, the ionic clusters show some peculiarities: they have special electronic structure and bonding properties in consequence of different interactions between the constituent atoms, ranging from genuine strong covalent bonds to weak van-der-Waals interactions, all this within a single aggregate and depending also on the electronic state. These features are closely related to the possibility of charge delocalization which is, however, *limited* to some well-defined parts of the clusters. This leads to characteristic geometric structures and dynamic behaviour. In addition to the general interest in studying such ionic clusters in the context of cluster physics and chemistry, another research motivation is that molecular or atomic ions surrounded by rare-gas atoms are appropriate models for solute-solvent aggregates [2,3]. Finally, to mention a more practical aspect, these complexes may arise in matrix investigations of molecular spectroscopy and processes.

Notwithstanding the considerable progress made both experimentally and theoretically, there is still only rather limited information available, even for small clusters of this kind. For medium-sized clusters very few theoretical studies have been published: several papers have treated pure cationic rare-gas aggregates, Rg_n^+, with n up to 35 (see, e.g., [4–18]) and corresponding protonated systems, Rg_nH^+, with n up to 7 [5, 19–22], using different approaches and resulting in partly contradictory findings. Recently also results of theoretical [23] and experimental [24] investigations of $Ar_nH_3^+$ complexes have been reported; the calculations ranged over n = 1–9. Somewhat more reliable and precise data are available for some small ionic complexes Rg_nM^+ with different rare-gas atoms Rg, different diatomics M and n = 1 or 2 (for references see, e.g., [25]). Almost nothing is known about the dynamics of such systems.

Because of this situation, systematic and well-founded investigations are desirable in order to understand structural, spectroscopic and dynamic properties of such

[a] e-mail: zuelicke@tc1.chem.uni-potsdam.de

clusters, and to make useful predictions which may even guide one to practical applications. In this vein, we started a study on simple prototype systems Rg_nM^+ and report here, in the first part, on the structure and binding of Ar_nH^+. In order to treat medium-sized clusters with reasonable effort, we choose a minimum basis diatomics-in-molecules (DIM) model for calculating the potential energy of interaction and other electronic properties (charge distribution) as a function of the geometric configuration.

The DIM approach has several important advantages: it guarantees correct asymptotic behaviour and can treat not only the electronic ground state but also low-lying excited states without additional effort. The computational expense is very low but the method requires extremely careful preparational work if it is to produce reliable results. Therefore, we have applied advanced ab-initio techniques to the task of obtaining the necessary input data, and we have checked the DIM results against refined conventional ab-initio calculations for a few small clusters at selected geometrical configurations.

The general aim of the project is twofold: firstly, we hope to provide an improved approach to finding a model which is able to treat both small and medium-sized molecular aggregates on the same footing in order to extend the results of the reliable quantum mechanical treatment of the very small systems to the region where ab-initio calculations are simply not feasible. Secondly, we should like to contribute to the understanding of structural aspects of the different-sized clusters, in particular to reveal, if existent, the building-up principle. Altogether this should give us the prerequisites for the future treatment of the dynamics of these clusters.

The procedure has recently been tested for the simple complex Ar_2H^+ [26] with encouraging results. In the present article, we extend our study to medium-sized clusters Ar_nH^+ with n up to more than 30. This is quite easily done, requiring minimal computational effort, even when some low-lying excited states are included; moreover, no new input data for the DIM model is needed over and above that already available from the work on Ar_2H^+ [26]. It is in this sense that the model we use here can be considered to treat all of the clusters on an equal footing.

The paper is organized as follows: in Section 2, the methodology for the pointwise generation of the interatomic-interaction potential energy in the conventional ab-initio approach and in the DIM model is briefly described. Section 3 summarizes the status of knowledge about the Ar_2H^+ complex and about the various diatomic fragments needed in the DIM scheme. It also reports on the results obtained for the Ar_nH^+ clusters, their structures and stability, including also some striking regularities observed. Finally, Section 4 contains the conclusions and an outlook.

2 Methodology of interatomic-interaction potential-energy calculation

The theoretical description of the systems under consideration is based on the adiabatic (Born-Oppenheimer) separation of electronic and nuclear degrees of freedom in its simplest version in which the potential-energy function governing the motion of the nuclei is given for each nuclear arrangement by the sum of the total energy of the electron cloud plus the total electrostatic nuclear repulsion energy. The essential problem to deal with is therefore the approximate solution of the electronic Schrödinger equation for a large set of nuclear configurations; this is done, for the most part of the paper, by an appropriate DIM model and, for purposes of cross-checking, by variants of the coupled-cluster approach (*vide infra*). In all calculations, the non-relativistic all-electron fixed-nuclei Hamiltonian in Cartesian coordinates is used. Relativistic effects do not play a role in the present case; in particular, there are no significant spin-dependent interactions.

A special problem for the larger clusters is to locate the relevant stationary points on the potential-energy surfaces (PES): local minima and first-order saddle points corresponding to (electronically) stable structures and transition configurations, respectively. To this end a Monte-Carlo procedure was applied to generate stochastically a large number of nuclear arrangements, each used for starting a steepest-descent optimization to find the nearest stationary point. Assuming a compact structure of the clusters, in the Monte-Carlo generation of initial geometries spherical polar coordinates for each atom are used, the values of which are appropriately connected with random numbers so as to ensure a homogeneous spatial distribution of all atomic positions within reasonable limits (e.g., no pair distances below 0.5 a_0). In order to avoid very large numbers of start geometries for larger clusters ($n > 13$ in the present case), the procedure has been modified so that not all atomic positions are freely randomly chosen, but the geometry of a smaller fragment of the cluster is preselected. In the subsequent optimization procedure which includes all degrees of freedom, Cartesian coordinates are used for practical reasons.

An overall fit of the PESs to analytic functions is not necessary because of the very short computational time needed by the DIM code; each PES point can be calculated immediately when it is required.

2.1 One-electron atomic basis sets

The elementary building blocks of the wavefunctions in each of the commonly used methods for solving the electronic Schrödinger equation are one-electron functions (orbitals) represented by linear combinations of appropriate atomic basis functions, mostly of Gaussian type. Various basis sets are proposed in the literature, differing in number and parametrization; we used the aug-cc-pVTZ basis set of Woon and Dunning [27] which includes, in addition to the set of Dunning [28], several diffuse functions, namely $1s$, $1p$, $1d$, $1f$ for Ar and $1s$, $1p$, $1d$ for H. According to our experience [29], this extended basis set (altogether $75n + 25$ functions, contracted to $50n + 23$ basis functions finally used in the calculations for Ar_nH^+) leads to a good compromise between sufficient flexibility and acceptable computational effort.

The incompleteness of any such basis set brings about a basis-set superposition error (BSSE). Its magnitude was estimated by the counterpoise method for a number of selected nuclear configurations of the diatomic fragments and the smallest complexes; it was found to be of the same order of magnitude (around 0.05 eV) as the errors from other shortcomings of the conventional ab-initio treatment, and less than the errors inherent in the DIM procedure applied (*vide infra*).

2.2 Conventional ab-initio MO-based configuration-interaction and coupled-cluster approaches

In the present study, all calculations of the electronic energy and wavefunction data of the diatomic fragments as well as the cross-checking reference data for selected structures of some polyatomic complexes are performed using a molecular-orbital (MO) configuration-interaction (CI) ansatz for the electronic wavefunction, i.e. a linear combination of a (very large) number of electronic (antisymmetric, spin-adapted) configuration-state functions built up from molecular orbitals which are represented, for their part, as linear combinations of the basis functions (*vide supra*). In order to generate electronic wavefunctions and continuous potential-energy curves of balanced accuracy (in particular with respect to maintaining an adequate representation of the dominant electronic configurations and including the essential higher one-electron excitations) over the whole range of internuclear distance for the diatomic fragments, the necessary flexibility in an unavoidably truncated CI function was achieved by using an internally contracted multi-reference single- and double-excitation variational configuration-interaction (icMRCI) procedure including a generalized Davidson correction for estimating the energetic contributions of higher-order excitations (icMRCI+Q) [30, 31]. For the single-point cross-checking calculations, a coupled-cluster approach with single- and double-excitations (CCSD) [32] was applied. All of these calculations were carried out with the MOLPRO suite of ab-initio programs [33].

For generating the best MOs for a given nuclear arrangement, a state-averaged complete active space self-consistent field (CASSCF) calculation was carried out prior to the MRCI step of computation. The active space of the CASSCF, consisting of the valence space plus the most relevant virtual orbitals, was then taken as the reference space in the MRCI. The inner-shell orbitals ($1s$, $2s$, and $2p$) of the argon atom are kept doubly occupied during the CASSCF and are treated as a frozen core in the MRCI and CCSD treatments.

For complexes Ar_nH^+ with $n > 2$, such ab-initio computations need so many of the resources that they become less and less feasible (for reasonable effort) as n increases. A much more economical alternative approach — the DIM model — is briefly described in the following section.

2.3 The diatomics-in-molecules (DIM) model

In 1963 Ellison [34] proposed a conceptually simple approach to solving the molecular electronic Schrödinger equation, based on the fact that the complete nonrelativistic fixed-nuclei Hamiltonian of an arbitrary N-atomic molecular system can be partitioned exactly into atomic and diatomic terms as follows:

$$\hat{H} = \sum_{a=1}^{N-1} \sum_{b=a+1}^{N} \hat{H}_{ab} - (N-2) \sum_{a=1}^{N} \hat{H}_a, \qquad (1)$$

where $\hat{H}_a$ contains contributions of atom a only, and $\hat{H}_{ab}$ includes all contributions from atoms a and b. The idea of Ellison, further worked out by Tully [35], Kuntz [36] and others, is to use many-electron wavefunctions for relevant electronic states of the constituent atoms and diatomic fragments (in contrast to most conventional methods which take MOs, i.e. one-electron functions, *vide supra*) as building blocks for the wavefunction of the total system. The latter is then set up in the form of a linear combination of functions each of which is a product of wavefunctions for atomic and diatomic fragments (neutral or ionic) in certain electronic states such that the resulting wavefunction belongs to a definite spatial symmetry and spin multiplicity of the electronic state of the total aggregate. The fragment wavefunctions, for their part, are thought of as being given by appropriate linear combinations of valence-bond (VB) functions, i.e. spin-adapted antisymmetric products of atomic orbitals (AOs).

In the present case, Ar_nH^+, if one takes into account all fragment states leading to singlet states of the whole complex and lying energetically not more than 10 eV above the respective fragment ground states, then one has to deal with the following fragment states:

$Ar(^1S)$, $Ar^+(^2P^\circ)$, $H(^2S)$,

$ArH(X^2\Sigma^+)$, $ArH^+(X^1\Sigma^+, 1^1\Pi, 2^1\Sigma^+)$,

$Ar_2(X^1\Sigma_g^+)$, $Ar_2^+(X^2\Sigma_u^+, 1^2\Pi_g, 1^2\Pi_u, 1^2\Sigma_g^+)$.

We will call this our "minimal" DIM model since it contains the smallest meaningful amount of fragment information. The set of wavefunctions for these states forms the "DIM basis".

It should be pointed out here that we restricted ourselves to this level of sophistication of the DIM approach in order to keep the computational expense low for calculating, in a subsequent study of the cluster dynamics, the PES points "on the fly".

Employing this wavefunction ansatz and the decomposition (1), the matrix elements of the Hamiltonian reduce to contributions from the isolated atomic or diatomic fragments in their different electronic states as selected above. These contributions can, in principle, be taken either from experimental data or from calculations. We use the latter way, applying extended conventional ab-initio calculations as described in the preceding section.

In the DIM approach, the wavefunction is much more compact (i.e., the linear combination ansatz is much shorter) compared to the MO-CI wavefunctions. This advantage, however, is achieved at the expense of extensive

preparational work: (a) the generation of the atomic and diatomic input data, (b) the conversion of these data into the form needed in DIM (namely, valence-bond-like wavefunctions), and (c) the composition of the matrix elements of the many-body Hamiltonian in terms of the 1-body atomic and the 2-body diatomic Hamiltonian matrix elements according to formula (1).

The treatment of problem (a) will be briefly described in the next section. Problem (b) is solved by a projection procedure, elaborated by Kuntz and Schreiber [37], which transforms each fragment wavefunction as obtained in the conventional MO-CI form (by MRCI) approximately into a single VB function or, if mixing of more than one VB configuration for the state considered is necessary, a linear combination of VB functions. It is important to note again that the MOs (in the MO configurations) and the AOs (in the VB configurations) are both represented as linear combinations of one and the same basis set (aug-cc-pVTZ in our case). We will not go further into details but mention only that this projection procedure requires merely the evaluation of determinants containing elements of the matrix of MO coefficients as obtained in the foregoing conventional ab-initio procedure. In this way we avoid carrying out independent expensive VB calculations for the diatomic fragment states as done in a large part of DIM work in the past. The step (c), including some approximations (in particular, neglect of overlap terms), is automatically executed in the DIM program code.

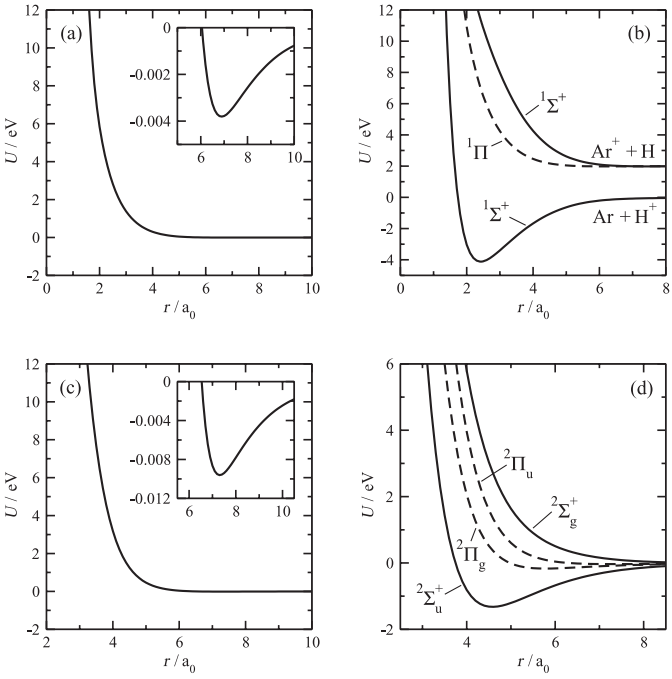

Fig. 1. Potential-energy curves for the relevant diatomic fragment states in the "minimal" DIM model: (a) ArH, (b) ArH^+, (c) Ar_2, (d) Ar_2^+ (taken from [26]).

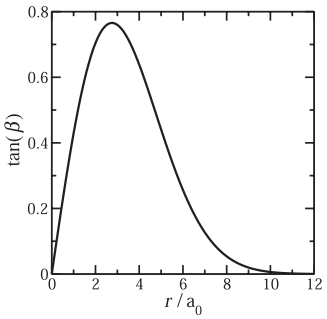

Fig. 2. VB configuration mixing ratio, $c_1/c_2 = \tan(\beta)$ where c_1 and c_2 are normalized coefficients of the ground and lowest excited $^1\Sigma^+$ states of ArH^+, respectively, in dependence on the internuclear distance (taken from [26]).

3 Results and discussion

3.1 Diatomic fragments

In order to provide the input data (the *parametrization*) for the DIM model described above, and to gain some insight into the relevant interatomic interactions in protonated argon clusters, we calculated the interaction potential-energy curves and electronic wavefunctions of the diatomic fragments in their lower electronic states (*vide supra*). Likewise, the electronic energies of the free atoms resp. ions, as far as included in the DIM basis, were determined. All this has been done by the ab-initio MRCI approach as specified in Section 2.2 above; the results for the potential-energy curves are given in Figures 1a–1d (see also [26, 29]).

For the electronic ground states of all four diatomic fragments, the electronic structure and binding properties are well known. The two ionic fragments, ArH^+ and Ar_2^+ (Figs. 1a and 1b) are firmly bound in their ground states with (electronic) dissociation energies D_e of 4.17 eV and 1.32 eV, respectively. The corresponding bond lengths r_e at the potential minimum are 2.42 a_0 and 4.58 a_0, and the harmonic vibrational frequencies ω_e amount to 2735 cm^{-1} and 300 cm^{-1}, respectively. All low-lying excited states considered are repulsive, as are the electronic ground states of the two neutral diatomic fragments, ArH and Ar_2. The repulsive states each exhibit some very weak long-range van-der-Waals attraction; the corresponding electronic binding energies are as low as a few meV: for example, 3.9 meV in the case of ArH and 9.7 meV for Ar_2 (without BSSE correction), and the interatomic distances at which the van-der-Waals minima appear, are 6.86 a_0 for ArH and 7.29 a_0 for Ar_2. All these diatomic fragment results compare well with experimental and theoretical data from the literature (see [29]).

In a VB-type approximate description, for the present selection of states, there occurs a mixing of the two $^1\Sigma^+$ states of the fragment ArH^+; this must be taken into account in the DIM model. The mixing coefficient of the two VB configurations as obtained by the projection procedure mentioned above, is shown in Figure 2. This result is very similar to earlier published findings (compare [38]). All the diatomic fragment data (interatomic potential energy including van-der-Waals bumps, mixing coefficient) as functions of the interatomic distance are carefully fitted to analytic (or spline) functions and used in this form as DIM input. The details will not be given here[1].

[1] More information can be obtained on request from one of the authors by e-mail: ritschel@chem.uni-potsdam.de

Table 1. Ground-state molecular characteristics of the most stable Ar_nH^+ cluster structures; upper line: CCSD[a] results, lower line: DIM results.

n	Symmetry/ Ground state	E_B^b eV	ZPE[c] eV	r_1^d a_0	r_2^d a_0	r_3^d a_0	α^d deg	q_H^e a.u.	q_1^e a.u.	q_2^e a.u.
2	$D_{\infty h}/^1\Sigma_g^+$	−4.73	0.162	2.84	–	–	180	0.328	0.336	–
		−4.57	0.164	2.76	–	–	180	0.635	0.182	–
3	$C_{2v}/^1A_1$	−4.81	0.166	2.84	6.13	–	178.3	0.343	0.326	0.005
		−4.65	0.167	2.77	5.97	–	176.1	0.635	0.182	0.001
4	$C_{2v}/^1A_1$	−4.89	0.171	2.84	6.12	7.50	177.3	0.364	0.314	0.004
		−4.75	0.172	2.77	5.93	7.27	173.6	0.636	0.181	0.001
5	$C_{2v}/^1A_1$	−4.98		2.84	6.17	7.48	177.5	0.384	0.304	0.004
		−4.84	0.177	2.77	6.05	7.25	174.0	0.635	0.181	0.001
6	$C_{2v}/^1A_1$	−5.06		2.84	6.20	7.51	178.7	0.397	0.297	0.004
		−4.93	0.181	2.78	6.14	7.29	176.4	0.635	0.181	0.001
7	$D_{5h}/^1A_1'$	−5.15		2.84	6.22	7.32	180	0.415	0.290	0.001
		−5.03	0.188	2.78	6.12	7.20	180	0.635	0.181	0.001

[a] For saving computer time, complete CCSD calculations have been carried out only for $n = 2$–4. [b] Binding energy: total energy relative to nAr + H^+. [c] Zero-point energy from harmonic frequencies. [d] Geometry: r_1 distance proton–Ar in the inner Ar_2H^+ fragment, r_2 distance proton–first ring Ar, r_3 distance first–second ring Ar, α bending angle of inner $(Ar–H–Ar)^+$ fragment. [e] Mulliken atomic charges: q_H - proton, q_1 - Ar atom of the inner Ar_2H^+ fragment, q_2 - first ring Ar atom (given are CISD data since CCSD charges cannot be calculated with MOLPRO).

3.2 The Ar_2H^+ complex

If not otherwise stated, we use Jacobi coordinates for defining the geometry of the triatomic complex Ar_2H^+: the Ar–Ar distance r, the distance R of the proton from the center of mass of the Ar–Ar pair, and the angle θ between the vectors $\boldsymbol{R}$ and $\boldsymbol{r}$ (see insert in Fig. 3b).

3.2.1 Electronic ground state of Ar_2H^+

As the starting stage of the present study, an extensive investigation of the simplest Ar_nH^+ complex, namely that with $n = 2$ in its electronic ground state, has been undertaken. For detailed information we refer to our recent paper [26] and give a brief summary here. Some data are collected in the upper two rows of Table 1.

In both the CCSD and the DIM approaches, the PES for the electronic ground state of Ar_2H^+ exhibits two local minima: one (Min1) for a centro-symmetric linear complex $(Ar–H–Ar)^+$, i.e. $D_{\infty h}$ symmetry, and one (Min2) for another linear arrangement $(Ar–Ar–H)^+$, i.e. $C_{\infty v}$ symmetry. Whereas the former is firmly bound by electrostatic and three-center covalent forces, the latter is only weakly stabilized by electrostatic interaction between one Ar atom and the ArH^+ molecular ion. These two local minima are separated by a saddle-point in a bent nuclear arrangement. The deeper minimum is clearly seen in the PES contour-line diagram given in Figure 3a. Even taking into account the zero-point vibrations, the two structures are still lower in energy than the fragmentation limit, but the barrier between them becomes nearly zero so that the weakly bound complex (Min2) will not play any significant role in the dynamics of the system. The qualitative similarity of the DIM and CCSD results provides a first justification for extending DIM to the study of larger complexes.

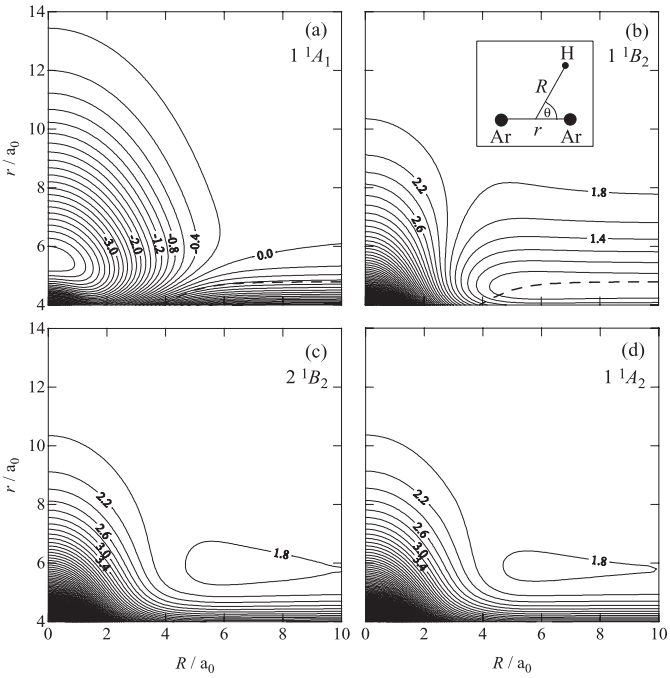

Fig. 3. DIM contour-line diagrams of the potential-energy functions $U(r, R)$ for the ground state and the first three excited states of Ar_2H^+ in C_{2v} symmetry: 1^1A_1, 1^1B_2, 2^1B_2, and 1^1A_2, respectively. The broken lines in the diagrams a and b indicate the crossing of the two lowest electronic PESs, 1^1A_1 and 1^1B_2.

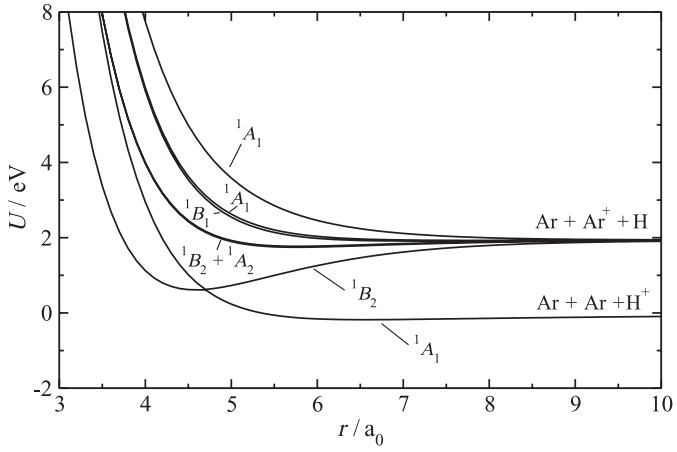

Fig. 4. DIM potential-energy curves $U(r)$ for the seven lowest electronic states of Ar_2H^+ in C_{2v} symmetry, keeping the distance R fixed at 6.0 a_0.

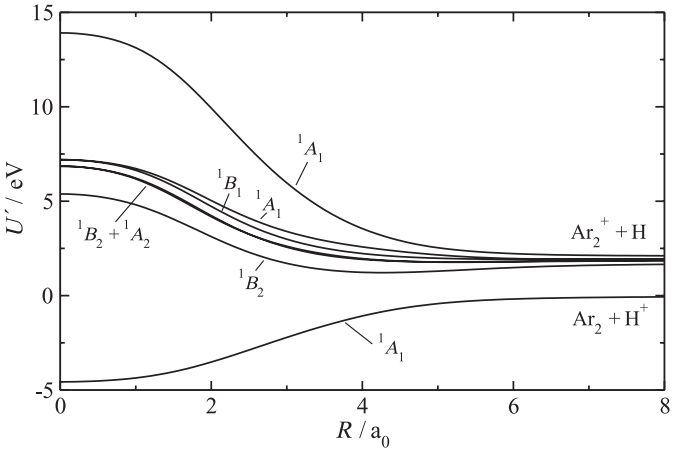

Fig. 5. DIM potential-energy curves $U'(R)$ for elongation of the Ar_2–H distance R in the seven lowest electronic states of Ar_2H^+, maintaining C_{2v} symmetry and optimizing the distance r for the electronic ground state.

Our findings confirm those in the literature which predict a centro-symmetric linear complex Ar_2H^+ as the most stable structure. There is no indication of a bent complex (as noticed in [22]) or of an asymmetric linear arrangement $(Ar–H\cdots Ar)^+$ with an ArH^+ core [21].

3.2.2 Low-lying excited states of Ar_2H^+

DIM can easily generate potential-energy surfaces for those excited states arising from the chosen basis. No additional input data or preparation is required, so that a certain number (depending on the basis-set dimension) of low-lying excited electronic states are available for free. In Figures 3a–3d the contour-line diagrams for the potential-energy functions $U(r, R)$ of the four lowest states are shown, keeping the Jacobi angle θ fixed at 90° (i.e., C_{2v} symmetry). Closer inspection and comparison of these pictures reveals the following interesting features, in addition to those already mentioned in the discussion of the electronic ground state: (i) all three excited states considered (we note: also the next higher ones) are clearly repulsive in the region vertically above the deeper minimum (Min1) of the ground-state PES. This is because the energy required to transfer electronic charge from Ar to the proton (the difference between the fragmentation limits Ar + Ar^+ + H and Ar + Ar + H^+ is about 2 eV) is not compensated by any attraction in the ArH^+ fragments. Indeed, one pays a large penalty in the form of repulsion between Ar^+ and H (see the excited-state curves in Fig. 1b); hence, there is an overall loss of attraction in the whole system. (ii) As can be seen from Figures 3a and 3b, the PESs of the two lowest electronic states cross in C_{2v}-symmetric nuclear configurations (but avoid crossing in general geometries, because both states then belong to the same symmetry species A′). The crossing is prominent in a region roughly defined by $r < 5$ a_0, $R > 3$ a_0 and $\theta \approx 90°$, as is further illustrated by Figure 4 representing a cut through the PESs for the seven lowest electronic states, laid one upon the other, keeping $\theta = 90°$ and $R = 6.0$ a_0 fixed. For Ar–Ar distances $r > 4.5$ a_0, the ground state has A_1 character, for $r < 4.5$ a_0 it has B_2 character. (iii) In each of these excited states, the PES may exhibit at least one shallow van-der-Waals well. For the first excited state, this well is largely obscured by the crossing seam; in the other two excited states shown in Figure 3, such wells are evident from the diagrams.

These special features of the PESs have obvious consequences: The repulsive nature of the excited states considered determines the behaviour of the Ar_2H^+ complex on photoexcitation. If the ground-state complex in its most stable structure is brought to one of these excited states, it will break up into ground-state atomic fragments. As far as excitation to the first excited state is concerned, the PES crossing may lead to a branching of the fragmentation channel into two: $Ar(^1S) + Ar^+(^2P°) + H(^2S)$, probably dominant, and $2Ar(^1S) + H^+$. The possible existence of electronically excited stable van-der-Waals complexes will not be pursued further because of the uncertainties of the calculated data (well depths and forms, corresponding zero-point energies) as calculated by the present DIM approach. What can be said, however, is that because of the large energy content of the complex after excitation, such van-der-Waals wells will not significantly affect the photofragmentation processes.

In order to get an overall picture of the electronic term structure relevant to the photoexcitation, potential-energy curves are shown in Figure 5 for the removal of the proton or, alternatively, the H atom, from the complex Ar_2H^+ in the lowest seven electronic states, maintaining C_{2v} symmetry and optimizing the Ar–Ar distance r in the electronic ground states at each value of R. Table 2 gives the electronic vertical spectrum, i.e. the electronic term energies relative to the bottom of the deepest ground-state potential well (most stable structure of the complex) as obtained from DIM and MRCI calculations, and also the transition-dipole matrix elements (TDME) computed

Table 2. Electronic vertical spectrum of Ar_2H^+ for excitation from the ground-state most stable structure ($X\,^1\Sigma_g^+$, Min1); upper line: MRCI+Q results, lower line: DIM results (in parentheses: symmetry of the correlating states for C_{2v}/C_s geometry).

state	ΔU^a	$\lvert\text{TDME}\rvert^b$
	eV	a.u.
$X\,^1\Sigma_g^+$ ($^1A_1/^1A'$)	0.0	–
ground state	0.0	–
$1\,^1\Pi_g$ ($^1B_2 + {}^1A_2/{}^1A' + {}^1A''$)	11.45	0.0
first excited state	11.42	
$1\,^1\Pi_u$ ($^1B_1 + {}^1A_1/{}^1A' + {}^1A''$)	11.81	0.05
second excited state	11.76	
$1\,^1\Sigma_u^+$ ($^1B_2/^1A'$)	12.39	2.20
third excited state	9.95	
$2\,^1\Sigma_g^+$ ($^1A_1/^1A'$)	16.32	0.0
fourth excited state	18.48	

[a] Vertical excitation energy. [b] Transition-dipole matrix element, for MRCI only.

with MRCI[2]. The DIM excitation energies are mostly in qualitative accordance with the MRCI results, except for the $1\,^1\Sigma_u^+$ state, which is above the two Π states for MRCI, and below for DIM. (We note here that in MRCI this state comes down somewhat as soon as the complex is bent and R increases; the discrepancy is then significantly reduced.) From the TDME data it follows that photoexcitation and, therefore, photofragmentation is effective mainly with the state $^1\Sigma_u^+$.

3.3 Structure and stability of medium-sized clusters Ar_nH^+ ($n > 2$)

If the necessary input data are available, the DIM procedure can be easily extended to larger Ar_nH^+ complexes; the computational effort is essentially determined by the diagonalization of the resulting $(3n+1)$-dimensional Hamiltonian matrix. We performed calculations up to $n = 35$. An increasingly time-consuming problem is the minimum search on the PESs for relatively large numbers of nuclear degrees of freedom and, correspondingly, large numbers of local minima. As mentioned at the beginning of Section 2, we applied a Monte-Carlo sampling of the relevant parts of the nuclear configuration space for initial choice of the structure, followed by a steepest-descent optimization procedure. If the number of such Monte-Carlo geometries is large enough to allow a sufficiently dense sampling of all essential parts of the potential-energy hypersurface (for medium-sized clusters this can easily require several thousand configurations), one can be sure to have discovered all important stationary points. In this way we found in each case not only the (electronically) most stable structure of the cluster (global minimum of the PES) but also some less stable secondary structures. Furthermore the harmonic frequencies have been obtained as well.

For the global minima of the smaller clusters with $n = 2$ (see preceding Section) up to $n = 7$ in their electronic ground states, starting from the DIM-optimized geometry, the optimization was repeated using the CCSD ab-initio approach, likewise (for $n = 2$–4) with determination of the harmonic frequencies, in order to check the minimum character of the stationary point and to estimate the zero-point energy (ZPE). In addition, to get some indication of the binding situation, the charge distribution is characterized by Mulliken atomic charges. The data obtained are used to extract the prominent regularities seen in building up the most stable cluster structures successively with increasing n.

The section ends with some remarks on the lowest electronically excited states of the clusters.

3.3.1 Electronic ground states: Building-up principle and increment scheme

A collection of structural and energetic data for the most stable nuclear arrangements of Ar_nH^+ clusters with $n =$ 2–7 in the electronic ground state appears in Table 1. The first interesting feature is the qualitatively good agreement of the DIM with the CCSD results for energetic and geometric-structure properties; this supports our concept for extending the DIM description further to cluster sizes which are not tractable by advanced ab-initio methods with reasonable effort. A marked discrepancy is observed for the atomic charges: DIM overestimates the charge on the proton but underestimates the charges on the Ar atoms (whereby practically all Ar atoms other than those of the Ar_2H^+ core are electrically neutral).

The most stable DIM structures of clusters with $n = 2$–35 are schematically drawn in Figure 6. One can see clearly that the successive formation of the clusters by adding one further Ar atom follows a simple building-up principle: beginning stepwise from Ar_2H^+, which is left essentially unchanged, a five-membered ring is formed in the equatorial plane (perpendicular to the Ar–H–Ar axis). When this ring is completed resulting in a symmetrical Ar_7H^+ structure a second five-membered ring is started on one of the two equivalent ends. After reaching the $Ar_{12}H^+$ structure, the most favourable place for an additional Ar atom is the "cap" position, not the position of a ring member on the other side. Only with Ar atom no. 14 is the formation of the next ring at the other end of the $(Ar–H–Ar)^+$ core initiated. Again the ring closure is followed by putting on the Ar "cap atom" no. 19. The cluster now looks like a "roller" made up of an axel with three wheels, the two outside wheels having hubcaps. By the way, the structures with $n = 7$, 12, 13, 18, and 19 agree with those obtained by using the van-der-Waals radii of Ar for finding the most stable clusters.

[2] Since the DIM approach does not employ wavefunctions explicitly, it does not allow for the determination of molecular properties such as TDMEs without much ado.

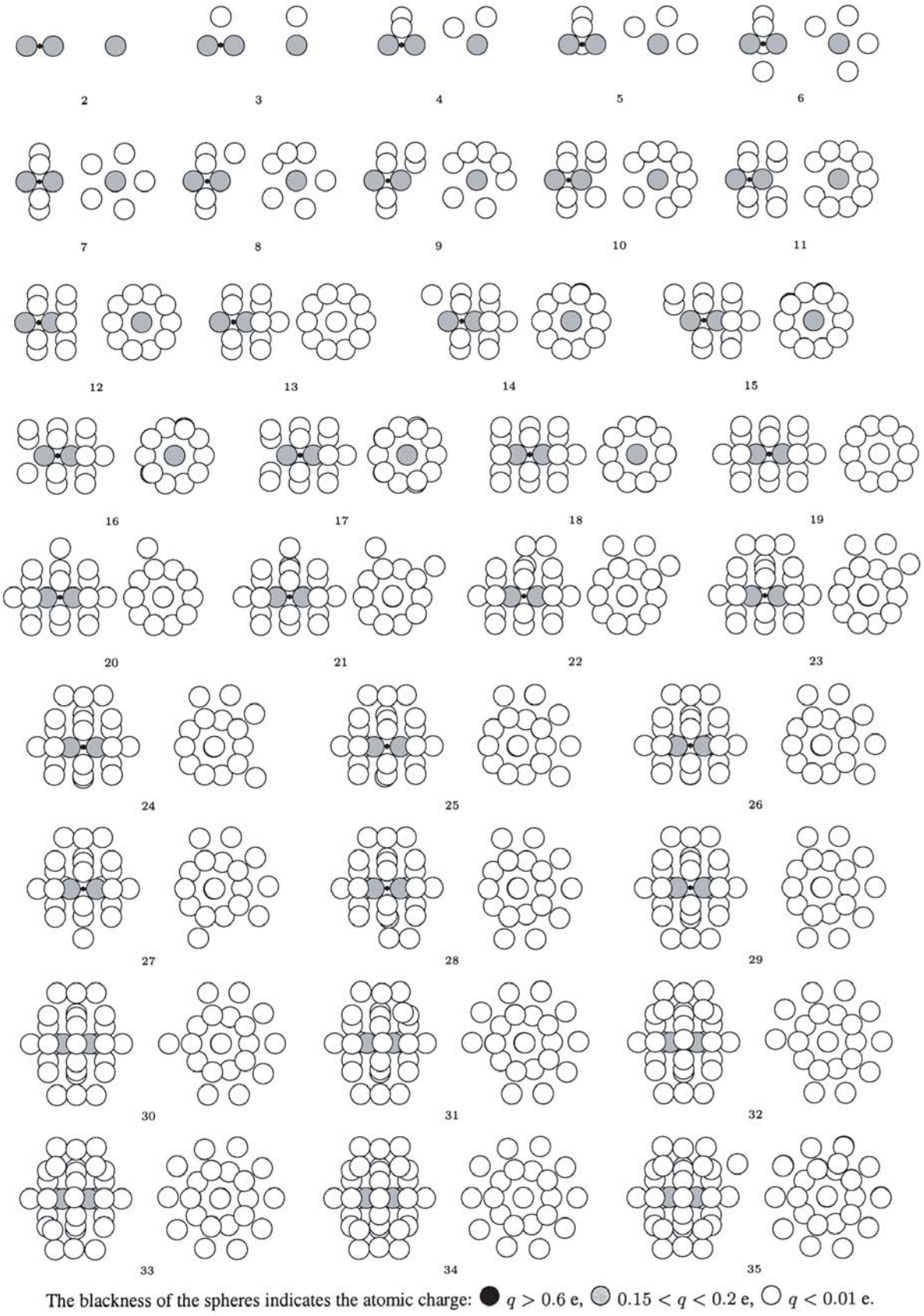

Fig. 6. The most stable Ar_nH^+ cluster structures with $n = 2$–35 as obtained with the DIM model, each in side view facing the $(ArHAr)^+$ core (left part) and end-on view along the $(ArHAr)^+$ axis (right part).

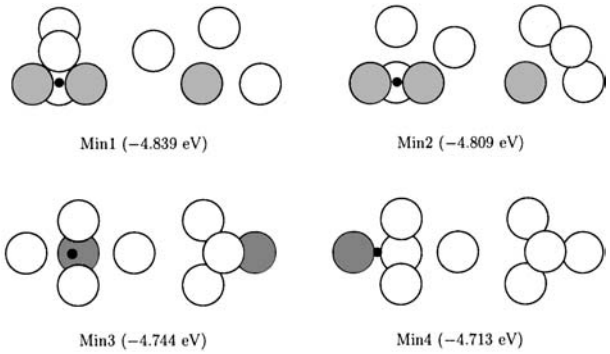

Fig. 7. The most stable and three less stable structures of the cluster Ar_5H^+, corresponding to secondary local minima on the ground-state PES. Two of the latter show clearly an ArH^+ core fragment with the Ar atom carrying a larger amount of charge ($q_1 = 0.32$ e with DIM).

From $n = 20$ onwards, extended "roller" clusters (made by adding extra 5-atom wheels to the axel) should exist as electronically stable aggregates, but they are no longer the most stable. Rather, a second shell of Ar atoms is built up, forming a 15-atom "tyre" around the 19-atom "roller", resulting in a complete "roller-with-tyre" cluster at $n = 34$. Let us consider this construction somewhat further in detail by inspecting the lower part of Figure 6. In a second shell around the central part again three five-membered rings are formed but now in a more complicated way. At first two neighbouring positions in the central equatorial plane are occupied ($n = 20$ and 21); this is to be expected because of the dominant inductive attraction forces exerted here by the core fragment. The following two Ar atoms ($n = 22$ and 23), however, are placed in the positions next to the former two on both sides (opposite on the gap), thus starting two new rings. In this way the procedure is continued: one Ar atom into the central ring next to the Ar atoms already present there, then two Ar atoms into the other two rings, one into each of them (n = 24–26, 27–29, and 30–32; now, the central ring is filled), and finally one Ar atom on each side to complete also the other two rings ($n = 33$ and 34). The Ar atom no. 35 finds its position in the shortest possible distance to the core fragment, near to one of the *cap* atoms of the $n = 19$ cluster. Presumably here another ring will be built up.

Without pursuing this cluster formation sequence to even larger numbers of Ar atoms, a progressively complicated competition of various imaginable, energetically nearly equivalent structures is to be expected in each case. In fact, for all clusters, a statistical mixture of such different cluster structures should exist, each structure corresponding to a local minimum on the PES. Some of these are shown in Figure 7 for the Ar_5H^+ aggregate. Here one observes, as in several other secondary structures, that the diatomic fragment ArH^+ can play the role of the core fragment.

The simple building-up procedure just described suggests that a correspondingly simple regularity should hold for the dependence of the energetic characteristics on the number n of Ar atoms. In Figures 8a and 8b graphs of the total binding (atomization) energy E_B,

$$E_B(n) = E(Ar_nH^+) - nE(Ar), \tag{2}$$

and the binding energy of the last added Ar atom (no. n) to the foregoing cluster $Ar_{n-1}H^+$ (the "evaporation energy"),

$$\begin{aligned} \Delta E(n) &= E(Ar_nH^+) - E(Ar_{n-1}H^+) \\ &= E_B(n) - E_B(n-1), \end{aligned} \tag{3}$$

as functions of n are shown. For n = 2–7 the DIM results are compared with the CCSD data. As can be seen, our DIM model systematically underestimates the absolute value of E_B and overestimates the amount of ΔE, but the tendency is remarkably well represented so that we again conclude that DIM can describe the cluster structures at least qualitatively correctly.

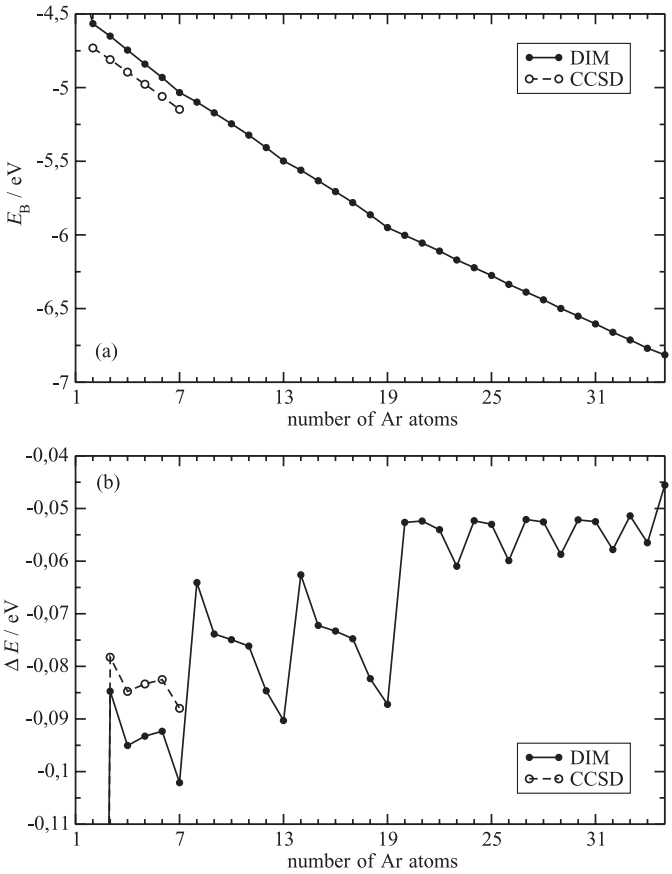

Fig. 8. Energetic characteristics of Ar_nH^+ clusters (most stable structures) as function of n: (a) total binding energy, E_B, (b) binding energy of the last added Ar atom, ΔE.

From Figure 8b, the "magic numbers" $n = 7$, 13, and 19, at which the rings (for $n = 13$ and 19 including the "caps") are complete and the clusters become most stable, are clearly discernible. Also for $n > 19$ we find some kind of "magic numbers", namely $n = 23$, 26, 29, 32, and 34. Possibly, beyond $n = 34$ this behaviour will change again.

The energetic regularities illustrated by Figures 8a and 8b result from the fact that, roughly speaking,

Table 3. Binding energy of Ar_nH^+ clusters with "roller-shaped" structure: comparison of the data from the additive increment scheme described in the text with those calculated individually by the DIM approach.

n	DIM	Increment scheme	ν_1	ν_2	ν_3	ν_4
	eV	eV				
2	−4.566	−4.566				
3	−4.651	−4.651	1			
4	−4.746	−4.746	2		1	
5	−4.839	−4.841	3		2	
6	−4.932	−4.936	4		3	
7	−5.034	−5.042	5		5	
8	−5.098	−5.104	5	1	7	
9	−5.172	−5.178	5	2	10	
10	−5.247	−5.251	5	3	13	
11	−5.323	−5.324	5	4	16	
12	−5.407	−5.408	5	5	20	
13	−5.498	−5.498	5	5	25	1
14	−5.560	−5.561	5	6	27	1
15	−5.632	−5.634	5	7	30	1
16	−5.706	−5.707	5	8	33	1
17	−5.781	−5.780	5	9	36	1
18	−5.863	−5.864	5	10	40	1
19	−5.950	−5.954	5	10	45	2

the interactions between an Ar atom and the rest of the cluster are of only two types, namely inductive (with the charged core atoms) and dispersive (with the other Ar atoms) showing additivity to a large extent. Thus it should be possible to formulate a simple increment scheme for the clusters as long as they obey a common building-up principle. To give an example, for $n = 3$–19 the binding energy (2) of the most stable structures can be adequately given by the following formula:

$$E_B(n) = E_{core} + \nu_1(n)\delta E_1 + \nu_2(n)\delta E_2 + \nu_3(n)\delta E_3 + \nu_4(n)\delta E_4. \quad (4)$$

Here ν_1 denotes the number of Ar atoms in the "central ring" (which is completed in Ar_7H^+), ν_2 the number of Ar atoms in the two "side rings", ν_3 the number of nearest-neighbour Ar–Ar pairs within the rings, and ν_4 the number of "cap" Ar atoms. The parameters (energy increments) as determined from the DIM energies for the most stable structures with $n = 2$, 3, 4, 12, and 13 (see Tab. 1), have the following values: $E_{core} = -4.5663$ eV, $\delta E_1 = -0.0847$ eV, $\delta E_2 = -0.0422$ eV, $\delta E_3 = -0.0103$ eV, and $\delta E_4 = -0.0387$ eV.

Using these parameters, the E_B for a given cluster with n Ar atoms is easily found by counting the numbers of the relevant interactions taken into consideration by the model chosen and summing up the corresponding energy contributions. As Table 3 shows, the results obtained agree very accurately with the data calculated by the DIM model; if we compare with Table 1, this holds also for the CCSD values. The trends in the energetic characteristics of Figures 8a and 8b are reproduced as well. It should be noted that, in our example, the increment scheme has been parametrized employing only a small part of the available data, thus demonstrating its predictive power within the given structural model.

Table 4. Electronic vertical spectrum of Ar_nH^+ clusters with $n = 3$–13 Ar atoms, for transitions from the most stable ground-state structures (DIM results) to the lowest five excited states.

n	first (1)	second (2)	third (3)	fourth (4)	fifth (5)
	eV	eV	eV	eV	eV
2	9.950	11.420	11.420	11.764	11.764
3	9.938	10.278	10.395	10.435	11.405
4	9.924	10.205	10.304	10.346	10.387
5	9.918	10.213	10.237	10.334	10.405
6	9.916	10.244	10.271	10.309	10.372
7	9.915	10.271	10.271	10.275	10.347
8	9.895	10.270	10.271	10.293	10.350
9	9.880	10.267	10.273	10.295	10.339
10	9.869	10.270	10.284	10.289	10.339
11	9.859	10.281	10.284	10.294	10.351
12	9.858	10.269	10.286	10.286	10.343
13	9.824	10.269	10.276	10.276	10.307

The less stable secondary structures mentioned above show marked differences to the most stable ones, but this behaviour will not be investigated further here.

It should be pointed out that the discussion in this section has focussed on the *electronic* stability of the aggregates. If we take into account the zero-point vibrations (for $n = 2$–7 estimated data are given in Tab. 1), the structures considered remain stable against fragmentation of any kind (e.g. break-up into smaller complexes, splitting-off of an argon atom), since the energy gained from adding an argon atom is considerably larger than the destabilization by the concomitant zero-point vibrational-energy contribution.

Finally we mention that the most stable protonated Ar clusters Ar_nH^+ exhibit remarkable structural analogies to the purely neutral counterparts Ar_n with the same n. We calculated the Ar_n structures on the same level of DIM as in the present study, i.e. with the Ar and Ar_2 data mentioned in Sections 2.3 and 3.1. Considering the smaller aggregates, the only exception is observed for $n = 6$: whereas Ar_6H^+ forms a pentagonal bipyramid with one missing corner (see Fig. 6), Ar_6 has octahedral structure (compare, e.g., also [39]).

3.3.2 Low-lying excited states of Ar_nH^+ ($n > 2$)

The low-energy part of the electronic term structure of medium-sized clusters Ar_nH^+ should, to a large extent, be similar to that found for the Ar_2H^+ complex (*vide supra*). Within the framework of the present study, it is not possible to pursue this in all detail. We show only some data which support the above-mentioned assumption. Table 4 (in extension to Tab. 2) gives for the clusters with $n = 3$–13 the vertical electronic excitation energies from the most stable ground-state configuration to the lowest five excited

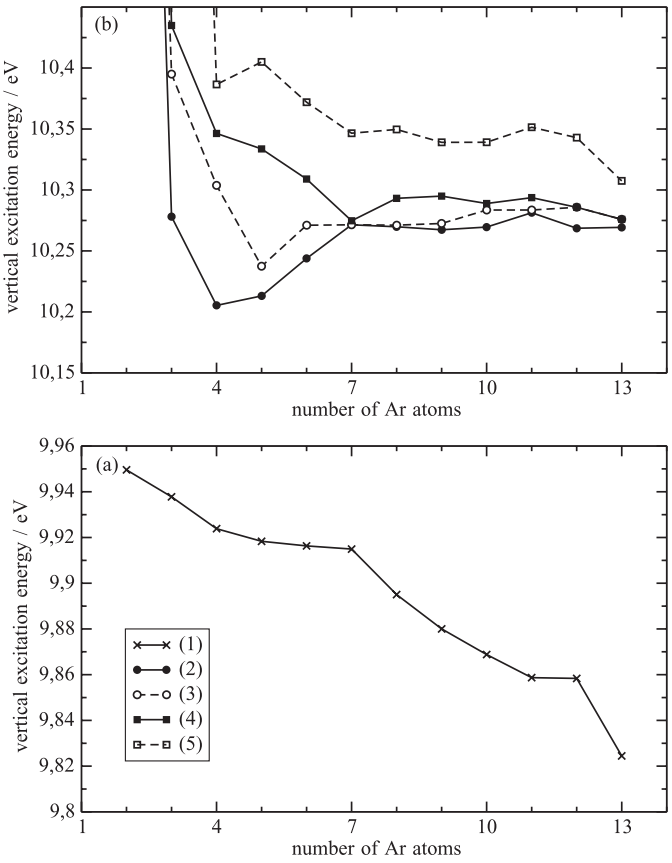

Fig. 9. Vertical transition energies from the electronic ground state (most stable structure) of Ar_nH^+ clusters (a) to the first excited state (longest-wave transition), (b) to the higher excited states up, in dependence on n.

states, calculated by means of the DIM approach. In Figures 9a and 9b the DIM vertical transition energies from the global minimum of the ground-states PES to the lowest five excited states are shown in their dependence on the cluster size (n). For the longest-wave transition (Fig. 9a), the points on the graph are, with the exception of the point for 12 Ar atoms, monotone decreasing over the range of n considered, whereas for the transitions to the higher excited states the vertical excitation energies tend to nearly constant values.

For the excited electronic states considered here, the asymptotic atomization limit is $(n-1)\mathrm{Ar}(^1\mathrm{S}) + \mathrm{Ar}^+(^2\mathrm{P}^\circ) + \mathrm{H}(^2\mathrm{S})$. The energy of the cluster after vertical excitation is in any case significantly higher than this asymptotic limit so that the result of photoexcitation can only be the complete fragmentation (atomization) of the cluster, as in the case of Ar_2H^+ already discussed in Section 3.2.2.

4 Conclusions and outlook

Based on the encouraging results for the Ar_2H^+ complex, the present article extends the study of the structure and binding to medium-sized clusters Ar_nH^+ using for the most part the diatomics-in-molecules (DIM) approach, which provides a uniform treatment of aggregates of all sizes, yielding information not only for the electronic ground state but also for some low-lying excited states. The methodical focus of the study is, on the one hand, to use the simplest meaningful DIM variant which can be justified by cross-checking with advanced conventional ab-initio calculcations for the smaller members ($n = 2$–7) of this class of clusters. On the other hand, the input data for this minimum DIM variant are very carefully prepared by accurate ab-initio computations of the diatomic fragments and application of a projection procedure.

The main findings can be summarized as follows:

1. comparison of the DIM results for the smaller clusters ($n = 2, \ldots, 7$) with coupled cluster ab-initio calculations shows that our "minimal" DIM model is able to describe adequately the geometry of the structures (at least the most stable ones) and the energetic relations between them. This increases our confidence that we have determined the relevant structures for the larger clusters as well;
2. analysis of the calculated structural and energetic data for the medium-sized Ar_nH^+ clusters reveals a building-up principle expressible as a simple relation between the energy of the most stable structure of each cluster and the cluster size, n; the parameters of this "increment scheme" succinctly encapsulate the DIM results, reproducing very accurately the results of the direct theoretical calculations;
3. the low-lying excited states calculated in the DIM approach are all globally repulsive, suggesting that photoexcitation processes should always lead to complete fragmentation (atomization). Clearly, the possible presence of shallow van-der-Waals minima in the excited-state potential-energy hypersurfaces (PESs) would be incapable of hindering this fragmentation.

The success of the "minimal" DIM model in describing the structural and energetic characteristics of medium-sized Ar_nH^+ clusters, together with the practical advantages of DIM, namely the much faster computation of PES points compared to all suitable conventional quantum-chemical methods, make the DIM model here ideal for generating plenty of PES data necessary for dynamical studies of processes involving the electronic ground state or excited states or both. We are planning further work in this direction.

References

1. T.A. Miller, V.E. Bondybey, *Molecular Ions: Spectroscopy, Structure, and Chemistry* (North-Holland, New York, 1983)
2. *Clusters of Atoms and Molecules*, edited by H. Haberland (Springer-Verlag, Berlin, 1994), Vols. I and II
3. *Reaction Dynamics in Clusters and Condensed Phase*, edited by J. Jortner, R.D. Levine, B. Pullman (Kluwer Academic Publishers, Dordrecht, 1994)
4. P.J. Kuntz, J. Valldorf, Z. Phys. D **8**, 195 (1988)
5. I. Last, T.F. George, J. Chem. Phys. **93**, 8925 (1990)

6. T. Ikegami, T. Kondow, S. Iwata, J. Chem. Phys. **98**, 3038 (1993)
7. F.Y. Naumkin, P.J. Knowles, J.N. Murrell, Chem. Phys. **193**, 27 (1995)
8. N.L. Doltsinis, P.J. Knowles, Mol. Phys. **94**, 981 (1998)
9. N.L. Doltsinis, P.J. Knowles, Chem. Phys. Lett. **301**, 241 (1999)
10. N.L. Doltsinis, P.J. Knowles, F.Y. Naumkin, Mol. Phys. **96**, 749 (1999)
11. N.L. Doltsinis, Mol. Phys. **97**, 847 (1999)
12. N.L. Doltsinis, P.J. Knowles, Chem. Phys. Lett. **325**, 648 (2000)
13. F.Y. Naumkin, D.J. Wales, Comput. Phys. Commun. **145**, 141 (2002)
14. D. Hrivňák, R. Kalus, Chem. Phys. **264**, 319 (2001)
15. P. Paška, D. Hrivňák, R. Kalus, Chem. Phys. **286**, 237 (2003)
16. R. Kalus, I. Paidarová, D. Hrivňák, P. Paška, F.X. Gadéa, Chem. Phys. **294**, 141 (2003)
17. R. Kalus, I. Paidarová, D. Hrivňák, F.X. Gadéa, Chem. Phys. **298**, 155 (2004)
18. R. Kalus, D. Hrivňák, Chem. Phys. **303**, 279 (2004)
19. M.E. Rosenkrantz, Chem. Phys. Lett. **173**, 378 (1990)
20. S.G. Potapov, L.P. Sukhanov, G.L. Gutsev, Russ. J. Phys. Chem. **63**, 479 (1989)
21. (a) F. Filippone, F.A. Gianturco, Europhys. Lett. **44**, 585 (1998); (b) F. Filippone, F.A. Gianturco, Phys. Chem. Chem. Phys. **1**, 5537 (1999)
22. K.T. Giju, S. Roszak, J. Leszczynski, J. Chem. Phys. **117**, 4803 (2002)
23. M. Kaczorowska, S. Roszak, J. Leszczynski, J. Chem. Phys. **113**, 3615 (2000)
24. M.K. Beyer, E.V. Savchenko, O.P. Balaj, I. Balteanu, B.S. Fox-Beyer, V.E. Bondybey, Phys. Chem. Chem. Phys. **6**, 1128 (2004)
25. L. Zülicke, F. Ragnetti, R. Neumann, Ch. Zuhrt, Int. J. Quantum Chem. **64**, 211 (1997)
26. T. Ritschel, L. Zülicke, P.J. Kuntz, Z. Phys. Chem. **218**, 377 (2004)
27. D.E. Woon, T.H. Dunning Jr, J. Chem. Phys. **99**, 3739 (1993)
28. T.H. Dunning Jr, J. Chem. Phys. **90**, 1007 (1989)
29. T. Ritschel, *Diploma Thesis*, University of Potsdam (1998)
30. H.-J. Werner, P.J. Knowles, J. Chem. Phys. **89**, 5803 (1988); P.J. Knowles, H.-J. Werner, Chem. Phys. Lett. **145**, 514 (1988)
31. P.J. Knowles, H.-J. Werner, Theor. Chim. Acta **84**, 95 (1992)
32. C. Hampel, K. Peterson, H.-J. Werner, Chem. Phys. Lett. **190**, 1 (1992) and references therein
33. MOLPRO is a package of ab-initio programs written by H.-J. Werner, P.J. Knowles, with contributions from R.D. Amos, A. Bernhardsson, A. Berning, P. Celani, D.L. Cooper, M.J.O. Deegan, A.J. Dobbyn, F. Eckert, C. Hampel, G. Hetzer, T. Korona, R. Lindh, A.W. Lloyd, S.J. McNicholas, F.R. Manby, W. Meyer, M.E. Mura, A. Nicklass, P. Palmieri, R. Pitzer, G. Rauhut, M. Schütz, H. Stoll, A.J. Stone, R. Tarroni, T. Thorsteinsson
34. F.O. Ellison, J. Am. Chem. Soc. **85**, 3540 (1963)
35. J.C. Tully, in *Modern Theoretical Chemistry*, edited by G.A. Segal (Plenum Press, New York, 1977), Vol. 7A
36. P.J. Kuntz, in *Atom-Molecule Collision Theory*, edited by R.B. Bernstein (Plenum Press, New York, 1979)
37. P.J. Kuntz, J.L. Schreiber, J. Chem. Phys. **76**, 4120 (1982)
38. P.J. Kuntz, A.C. Roach, J. Chem. Soc. Faraday Trans. 2 **68**, 259 (1972)
39. The Cambridge Cluster Database, D.J. Wales, J.P.K. Doye, A. Dullweber, M.P. Hodges, F.Y. Naumkin, F. Calvo, J. Hernández-Rojas, T.F. Middleton, `http://www-wales.ch.cam.ac.uk/CCD.html`